Journal of Arid Environments 131 (2016) 25–34

Contents lists available at ScienceDirect

Journal of Arid Environments

journal homepage: www.elsevier.com/locate/jaridenv

A multi-scale approach to assess the effect of groundwater extraction on *Prosopis tamarugo* in the Atacama Desert

Mathieu Decuyper [a, b, *], Roberto O. Chávez [c], Paul Copini [a, d], Ute Sass-Klaassen [a]

[a] Forest Ecology and Forest Management Group, Wageningen University, Droevendaalsesteeg 3, 6708 PB Wageningen, The Netherlands
[b] Laboratory of Geo-Information Science and Remote Sensing, Wageningen University, Droevendaalsesteeg 3, 6708 PB Wageningen, The Netherlands
[c] Institute of Geography, Pontificia Universidad Católica de Valparaíso, Valparaiso, Chile
[d] Vegetation, Forest and Landscape Ecology, Alterra, Wageningen UR, Droevendaalsesteeg 3, 6708PB, Wageningen, The Netherlands

ARTICLE INFO

Article history:
Received 6 July 2015
Received in revised form
25 March 2016
Accepted 28 March 2016

Keywords:
Groundwater depletion
Dendrochronology
Remote sensing
NDVI
Drought
Multi-scale approach

ABSTRACT

Groundwater-dependent ecosystems occur in arid and semi-arid areas worldwide and are sensitive to changes in groundwater availability. *Prosopis tamarugo* Phil, endemic to the Atacama Desert, is threatened by groundwater overexploitation due to mining and urban consumption. The effect of groundwater depletion on two representative sites (low -and high-depletion) was studied using a multi-scale approach, combining remote sensing based estimations of canopy growth and water condition, and tree-ring based analysis of stem growth. On the stand level two NDVI (Normalized Difference Vegetation Index) -derived parameters: NDVI in winter and the difference between NDVI in summer and winter showed significant negative trends in the high-depletion site, indicating drought stress. Radial stem growth of viable *P. tamarugo* trees was 48% lower in the high-depletion site. At the tree level, the Green Canopy Fraction (GCF) also indicated drought stress since a larger percentage of trees fell within lower GCF classes. Groundwater depletion of 3 m, reaching a groundwater depth of >10 m, increased drought stress, and led to reduced growth in viable trees. Viable trees may be able to adapt to the drop in groundwater levels by increasing root growth, whereas for non-viable trees, the effects might be detrimental.

1. Introduction

Groundwater-dependent ecosystems occur in semi-arid and arid areas in the Americas (Bogino and Jobbágy, 2011; Stromberg et al., 1996), Africa (February et al., 2007), Asia and Australia (Zencich et al., 2002). Although perfectly adapted to harsh environments, the vegetation is susceptible to natural or anthropogenic changes in groundwater sources (Eamus et al., 2015; Jobbágy et al., 2011; Naumburg et al., 2005). Globally these ecosystems are threatened by excessive groundwater extraction, which causes partial crown dieback (Cooper et al., 2003), or even mortality in trees (Groom et al., 2000) and changes in ecosystem functions and structure (Eamus et al., 2015). This is especially true for phreatophyte species in arid environments, which is why in order to conserve such ecosystems it is crucial to understand the response of these species to drought (Eamus et al., 2015). Perhaps the most extreme case of adaptation to arid environments is the endemic phreatophyte tree *Prosopis tamarugo* Phil. This thorny tree is one of the few tree species able to survive in the hyper-arid Atacama Desert in Northern Chile, a place considered one of the most extreme places on Earth to sustain life (McKay et al., 2003; Navarro-González et al., 2003). This protected species is found in forested areas, locally known as Pampa del Tamarugal, where the groundwater table is relatively shallow; between 4 and 18 m below ground (Altamirano, 2006; Acevedo and Pastenes, 1983). In this ecosystem, besides some exceptional rain events groundwater aquifers are the only source of water, which are fed by the rainfall, glaciers and snowmelt from the Andes mountain range (Favier et al., 2009;

* Corresponding author. Laboratory of Geo-Information Science and Remote Sensing, Wageningen University, Droevendaalsesteeg 3, 6708 PB Wageningen, The Netherlands.
E-mail addresses: mathieu.decuyper@wur.nl (M. Decuyper), roberto.chavez.o@gmail.com (R.O. Chávez), paul.copini@wur.nl (P. Copini), ute.sassklaassen@wur.nl (U. Sass-Klaassen).

http://dx.doi.org/10.1016/j.jaridenv.2016.03.014
0140-1963/

Gascoin et al., 2011; Rojas and Dassargues, 2007). Rojas and Dassargues (2007) also identified the pumping of groundwater as the main driver of (negative) groundwater level changes.

The Pampa del Tamarugal basin (21°07′S, 69°26′W) is one of the most important sources of groundwater within an area of about 4200 km^2 (DICTUC, 2008; Rojas and Dassargues, 2007; Rojas et al., 2010). Authorized groundwater extraction that started in 1988 in this area steadily increased, reaching 4000 l/s in 2012, which is four times the estimated natural recharge (CIDERH, 2013; DICTUC, 2008, 1988; JICA-DGA-PCI, 1995; Rojas and Dassargues, 2007; Rojas et al., 2010). The consequence has been a steady fall of the groundwater table throughout the whole aquifer, especially in areas close to extraction wells. Further lowering of the groundwater level as a result of groundwater extractions could threaten the survival of *P. tamarugo* (Chávez et al., 2016).

The effects of groundwater extraction on *P. tamarugo* trees have been studied using remote sensing tools, ranging from experiments to large scale spatio-temporal studies using satellite images (Chávez et al., 2013a,b, 2014, 2016). However, this spatio-temporal assessment, as many other remote sensing based studies, was focused on the retrieval of canopy parameters only. In this contribution, remote sensing based estimations of *P. tamarugo* canopy growth and its water condition were combined with tree-ring based analysis of *P. tamarugo* stem growth. For temporal drought assessments, tree-ring analysis has been used to assess both short- and long-term effects of groundwater depletion on the growth of desert trees (Stock et al., 2012). Prosopis species are known to form annual rings in response to seasonal changes in water availability (Bogino and Jobbágy, 2011; López et al., 2008; Rivera et al., 2010; Villalba and Boninsegna, 1989), and in the case of *Prosopis flexuosa* DC. drought stress led to a decrease in radial growth or the ring-width (Giordano et al., 2011). By analysing these two data streams (i.e. remote sensing and tree-ring analysis), drought stress can be assessed in this species by considering two main carbon allocation pools together (crown and stem). Currently it is not known how the crown parameters obtained via satellite data relate to stem growth. A multi-scale approach combining data from different data sources and scales (Normalized Difference Vegetation Index in winter, difference of winter and summer Normalized Difference Vegetation Index and tree-ring research on plot level, and Green Canopy Fraction on tree level) was used to assess the impact of groundwater depletion on *P. tamarugo*.

The following hypothesis was tested: trees at a site with high groundwater depletion (about 3 m) will show drought stress symptoms which can be captured by both dendrochronological (decrease in ring-width) and decrease in the remote sensing parameters. Two contrasting sites with and without groundwater depletion, were studied to answer the following questions:

(1) Is there a reduction in radial growth at the site with groundwater depletion?
(2) How do stress indicators of drought assessed by remote sensing (crown status) relate to information obtained from dendrochronology (ring-width)?
(3) Finally, can high spatial resolution remote sensing analysis (Green Canopy Fraction on tree level) provide further insight on the drought assessment at the stand level?

To the authors' knowledge this approach combining remote sensing with dendrochronology has not previously been applied in tropical or subtropical areas to detect drought stress in groundwater-dependent ecosystems.

2. Material and methods

2.1. Species description

The endemic and protected *Prosopis tamarugo* Phil. belongs to the Leguminosae family and is one of 44 species of the *Prosopis* genus (Burkart, 1976). This evergreen species often forms multiple stems with an average diameter of 0.5–0.8 m and heights of 20–25 m, and is adapted to high saline conditions (Altamirano, 2006; Briner, 1985). It has thorny branches and a crown width of up to 20 m (Fig. 1a) (Altamirano, 2006). The *P. tamarugo* has fast juvenile growth, reaching heights of 2–2.5 m in 3–5 years (Botti and Sudzuki, 1970). Field experiments have found that roots of seedlings quickly reach 0.8–1.2 m when shoots are only 6–8 cm long (Sudzuki, 1985a). The root system consists of dense lateral superficial roots with a large tap root branching out and reaching depths up to 12–18 m (Mooney et al., 1980; Sudzuki, 1985b; Acevedo and Pastenes, 1983). Chávez et al. (2016) indicated that roots may reach a depth of 20 m. Partial foliage loss may occur between May and September (winter) and Ortiz et al. (2010) estimated a maximum foliage loss of 30% in the absence of drought stress before new leaves appear in September. *P. tamarugo* wood is very dense, with many resin ducts to protect the wood tissue after possible injury. The stem has a large area of dark-brown hardwood and a small band of pale sapwood. The wood is similar to that of *P. flexuosa* DC (Giantomasi et al., 2013; Villagra et al., 2005; Villalba, 1985) and *Prosopis alpataco* (Villagra and Roig, 1997) with a diffuse-porous vessel structure and tree-ring boundaries indicated by terminal parenchyma bands (Fig. 1c).

2.2. Sampling sites and groundwater data

P. tamarugo is mainly distributed in the Pampa del Tamarugal basin; almost 160 km long, with a width of 20–60 km (Fig. 2a) and ~1000 m above sea level (Rojas and Dassargues, 2007). The Pampa del Tamarugal aquifer is fed by groundwater from the eastern subbasins where annual precipitation is about 200 mm (Aravena, 1996). Sampling was conducted in the Pintados plantations in the Pampa del Tamarugal aquifer located in a National Reserve where establishment began in 1971 (CONAF, 1997) (Fig. 2a). The Pintados plantations are located in the heart of the hyper-arid Atacama Desert in northern Chile, which is characterized by high temperatures (up to 45 °C), a potential evaporation rate of 145 l/s year^{-1}, and transpiration rate of 904 l/s year^{-1} (JICA-DGA-PCI, 1995; Rojas and Dassargues, 2007), virtually zero precipitation (Houston and Hartley, 2003; Houston, 2006) and the absence of vegetation cover across vast areas. Since groundwater levels are close to the surface in some areas, high evaporation causes salt accumulation in the upper layers of the soil (Houston, 2006).

P. tamarugo seedlings had been planted (around 1971) in holes of ~60 cm deep after removal of the salt crust (40 cm) and irrigated until establishment (Habit et al., 1981). Based on the results of Chávez et al. (2016) showing an increasing drought stress towards the south and east of the Pampa del Tamarugal aquifer, two contrasting sites were selected with i) different groundwater extraction rates (given by actual measures of groundwater level, i.e. close to monitoring wells), ii) similar initial groundwater levels before the major water extraction event, and iii) plantations with only *P. tamarugo* trees (not mixed with other species) with similar plantation years. The low-depletion site had very little depletion (0.4 m) and is 0.47 km^2 and the high-depletion site had around 3 m groundwater depletion and is 0.33 km^2 (Figs. 2b and 3a). Although some private plantations outside the CONAF reserve presented higher depletion (two wells) than the selected high-depletion site, they were ignored, since the advantage of the CONAF stands is that

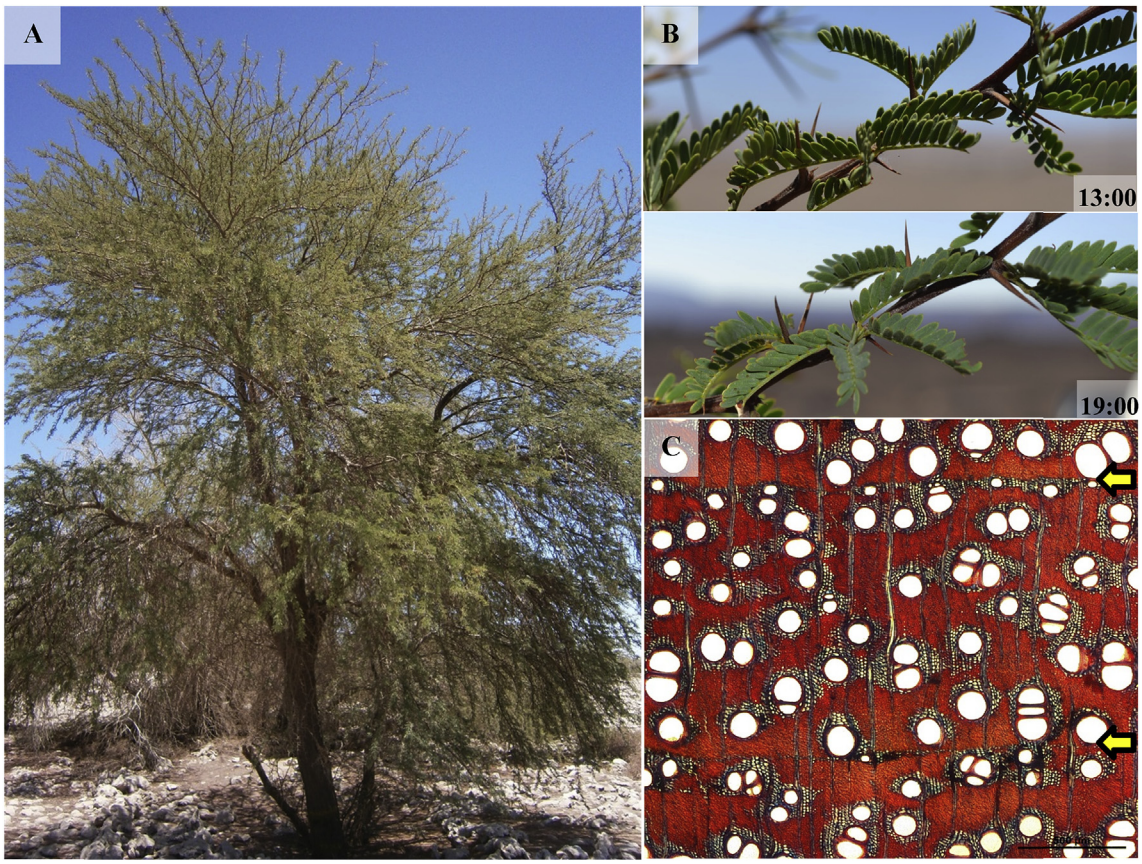

Fig. 1. (A) *Prosopis tamarugo* Phil. in the Pintados plantation. (B) Paraheliotropic leaf movements with leaves in erectophile position at midday to avoid excess light and drought stress (top) and in planophyle position in the evening. (C) Micro section of the stem wood, showing two annual ring boundaries (see arrows). The ring boundaries are depicted by small bands of marginal parenchyma (see also Fig. A in the supplementary results).

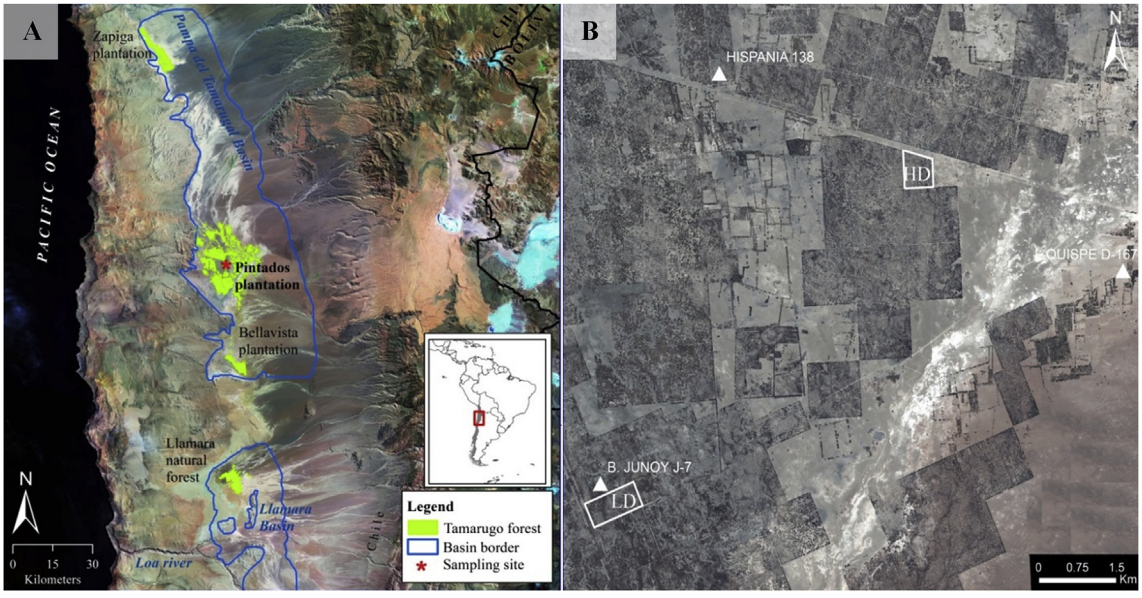

Fig. 2. A) Landsat composite showing the Pampa del Tamarugal basin and the location of the *P. tamarugo* forest stands (green). B) True colour high spatial resolution image showing the low- (LD) and high-depletion (HD) sites and monitoring wells (triangles). (For interpretation of the references to colour in this figure legend, the reader is referred to the web version of this article.)

the approximate age of the trees is known, and this is crucial for tree-ring studies (CONAF, 1997; Habit et al., 1981). In the past both the low-depletion and high-depletion sites had groundwater tables at similar depths: in 1989 the groundwater level (GWL) in the

monitoring wells in the high-depletion site was similar to that in the wells in the low-depletion site (i.e. 8–9 m depth). In 1990 groundwater extraction for mining and urban use began near the high-depletion site (Rojas and Dassargues, 2007; Rojas et al., 2010). No groundwater extraction occurred near the low-depletion site and the GWL remained almost constant over time. There was no forest management conducted at our study sites after tree establishment.

All available GWL data from the monitoring network of *Dirección General de Aguas* (DGA), spanning the period 1987–2012 was used. One monitoring well is within the low-depletion site: Jica 7 (B. Junoy J–7) (20°30′S, 69°40′W). Two monitoring wells are near the high-depletion site: Felix Quispe (Quispe D–167) (20°27′S, 69°34′W) and Planta AP Hispania (Hispania 138) (20°27′S, 69°38′W, Fig. 2b). The GWL in the high-depletion site was obtained by using inverse distance weighting spatial interpolation in ArcMap (version 10.2.1) over a 10 × 10 m grid of the monitoring wells Quispe D–167 and Hispania 138, which are east and west respectively of the site (Fig. 2b). Mean annual GWL in metres below ground level (i.e. negative values) was used. Although solar radiation and temperature showed seasonal changes, the seasonal patterns are constant over time (i.e. no trends), and precipitation is negligible (Houston, 2006; Rojas and Dassargues, 2007), thus these data were not used in the study.

2.3. Measurements

2.3.1. Dendrochronological sampling and analyses

Since the *P. tamarugo* trees are endangered and protected dendrochronological sampling was restricted to stem disks of eight trees in the low-depletion site and four trees in the high-depletion site, under the supervision of the Chilean forest service CONAF. Stem disks just above the soil surface level were collected from multi-stemmed trees in March 2012 in such a way that sampled trees retained enough crown to reach crown closure again in the future. Only viable trees (GCF class 75–100, this crown classification is explained in section 2.3.2) were selected and a dominant straight stem was chosen, to avoid bias in ring-width due to competition. The sampled trees were approximately seven metres high with stem diameters from 8 to 22 cm. All stem disks were air dried and sanded using a sequence of sandpaper of decreasing grit size up to grade 1000 (López et al., 2008). Tree-rings were identified under a stereo microscope at a magnification between 8 and 100× (Leica MZ 12.5). Tree-rings or ring-widths (RW) were measured along three radii per stem disk and crossdated visually (WinTSAP©) and statistically (WinTSAP©, COFECHA) (Holmes, 1983). The Expressed Population Signal (EPS) and Species intercorrelation (Rbar) were calculated. The EPS provides an estimate of how well the mean chronology based on a finite number of trees fits the hypothetically perfect chronology based on an infinite number of trees. The EPS value is between 0 and 1, and values above 0.85 are generally assumed to indicate a good fit (Wigley et al., 1984). The Rbar indicates how well the individual ring-width series are intercorrelated, with high values indicating high correlations. For time-series analysis the R statistical package dplR (R development Team) was used (Bunn, 2008). Mean chronologies were calculated for both sites (López et al., 2005) and subsequently related to groundwater level and the remotely-sensed Normalized Difference Vegetation Index in winter (NW) and difference of winter and summer Normalized Difference Vegetation Index (NWSD) (explained in Section 2.3.2). Detrending was not applied since the time series were too short and statistical modification of the ring-width series would have complicated the comparison with the long-term variation in groundwater level (Grissino-Mayer, 2001). The fast growing rate during the juvenile phase of about 15 years (see Results and Fig. B of the Supplementary materials) was excluded from the analysis to avoid the ontogenetic effect.

2.3.2. Remote-sensing data

2.3.2.1. Landsat – NDVI derived metrics for paraheliotropic plants. *P. tamarugo* is a paraheliotropic plant, i.e. its leaves adapt their inclination angle to avoid excessive solar radiation and photoinhibition (Ehleringer and Forseth, 1980), as shown in Fig. 1b. In this way, paraheliotropic plants can photosynthesize longer than normal plants under high solar radiation (Pastenes, 2004). At the peaks of solar radiation their leaves fold, avoiding the solar rays and causing a drop in the canopy's spectral reflectance and NDVI (Chávez et al., 2014, 2013b). These authors showed annual NDVI time series of *P. tamarugo* stands with peaks in winter and drops in summer, which were negatively correlated to in-situ measured solar radiation (Chávez et al., 2013a, 2014). Based on this annual behaviour of NDVI, Chávez et al. (2014), proposed new indices for paraheliotropic vegetation: the mean NDVI in winter (NW) as an indicator of annual green biomass (thus expected to decrease over time in case of drought stress) and the NDVI difference between summer and winter (NWSD) as an indicator of the normal paraheliotropic movement and thus an indicator of canopy water content. Trees under drought stress are no longer able to perform paraheliotropic leaf movements, since water is needed for the pulvinus to function, thus the difference between NDVI in winter and summer will be minimal (and therefore lower than in non-drought stressed trees). In addition the NWSD is expected to decrease over time in stressed trees. In this paper, we used both NW and NWSD indices for annual estimations of green biomass and canopy water content of *P. tamarugo* stands.

For the two study sites, all available Landsat 5 TM (Thematic Mapper) and Landsat 7 ETM (Enhanced Thematic Mapper – inclusive the SLC-off scenes) satellite data covering the period 1989–2012 were downloaded from the USGS Earth Explorer website and were considered for use. For the Landsat NDVI time series, cloud-free L1T (orthorectified and geo-referenced) images of 30 m pixel resolution (471 scenes, corresponding to path 1 and row 34) were used. The images were pre-processed using the Landsat Ecosystem Disturbance Adaptive Processing System (LEDAPS) to obtain surface reflectance values for all spectral bands (Masek et al., 2006). Finally, the surface reflectance values of the red band and NIR Near Infra-Red (NIR) band were used to compute the NDVI for each date via the following algorithm: NDVI = (NIR-Red)/(NIR + Red). The median NDVI values of all pixels within the plot were calculated. There was no significant seasonal behaviour related to BRDF (bidirectional reflectance distribution function) effects (Chávez et al., 2014). Annual values of NW and NWSD were calculated as average pixel values within both sites:

(1) NW = average of all NDVI scenes from May, June and July (midwinter);
(2) NWSD = NW – NS, where NS = average of all NDVI scenes from November, December and January (midsummer).

In total, 522 and 367 Landsat pixels were used for the low- and high-depletion sites respectively. To obtain representative values for NS and NW, only years with at least three images in the period June–July–August (midwinter) and November–December–January (midsummer) were used to calculate the average per season (i.e. no intra-annual data, but one value per year).

2.3.2.2. Very high spatial resolution (VHSR) satellite images – Green Canopy Fraction (GCF).

At the single tree level, other indicators derived from satellite

data can be used as drought indicators. Via high spatial resolution satellite images, the Green Canopy Fraction (GCF) from individual *P. tamarugo* trees can be obtained (Chávez et al., 2016). It has been shown that drought stress causes *P. tamarugo* to loose canopy over time (Chávez et al., 2013b), thus GCF is expected to decrease. The GCF values provide information on the status of the crown viability (an indirect measurement of photosynthetic activity) at tree level.

The GCF was calculated as the ratio of green to brown parts of the canopy (green canopy/(green + brown canopy)) assessed from four angles at ground level (digital photos) and was related to the spectral signal of a Worldview2 image of 2 m pixel resolution from July 2011. Single tree canopies were delineated with a Quickbird2 image in summer (to avoid crown shadows) with a 0.6 m pixel resolution (Chávez and Clevers, 2012). The GCF was divided into four classes (each of 25%), starting with the class < 25%, which represents trees with a very dry canopy.

2.4. Statistical analyses

2.4.1. Stand level variables (GWL, NW, NWSD, RW)

For the stand level comparison, the Mann–Kendall trend (MKT) test as suggested by Hipel and McLeod (1994) and later by De Beurs and Henebry (2005) was used to check for significant trends on the monotonic series of annual GWL (expressed in negative values), annual RW, NW, NWSD. Temporal stationarity was accomplished in most cases, as shown by the autocorrelation function (ACF as implemented in the R package). The only significant autocorrelation found was for the GWL series for the high-depletion sites and for time lags of < 4 years. Association between different time series was analysed by the Kendall rank correlation (KRC). The analysis was performed using the Kendall package of R and significance levels of 0.01, 0.05 and 0.1 were shown. Additionally differences between the mean values of each parameter (RW, NW, NWSD and GWL) per site were calculated, using all annual time steps as single replicates and assuming independent samples as shown by the ACF function. Since some of the parameters were not normally distributed the non-parametric Mann-Whitney *U* test (using IBM SPSS Statistics 22 software) was used for all parameters to compare the variables at each site.

2.4.2. Single tree variables (GCF)

GCF was used to describe the cumulative effect of drought stress on the amount of remaining green canopy of single trees at both high-depletion and low-depletion sites. For this variable the non-parametric Mann-Whitney *U* test was also used to test differences between the GCF values at the two sites using single trees as replicates.

3. Results

3.1. Groundwater level

The GWL dropped by 0.4 m in the low-depletion site (data available for 1987–2012) and ~3 m in the high-depletion site (data available for 1989–2012). While the decreasing trend of the high-depletion site was highly significant ($p < 0.01$), the significant decreasing trend in the low-depletion site was less strong ($p < 0.05$), as shown by the Mann-Kendall trend test (i.e. the decreasing trend of the high-depletion site was more evident). The GWL of the high-depletion site was significantly lower than the low-depletion site ($U < 0.001$; $Z = -6.059$; $p < 0.001$) according to the Mann-Whitney *U* test.

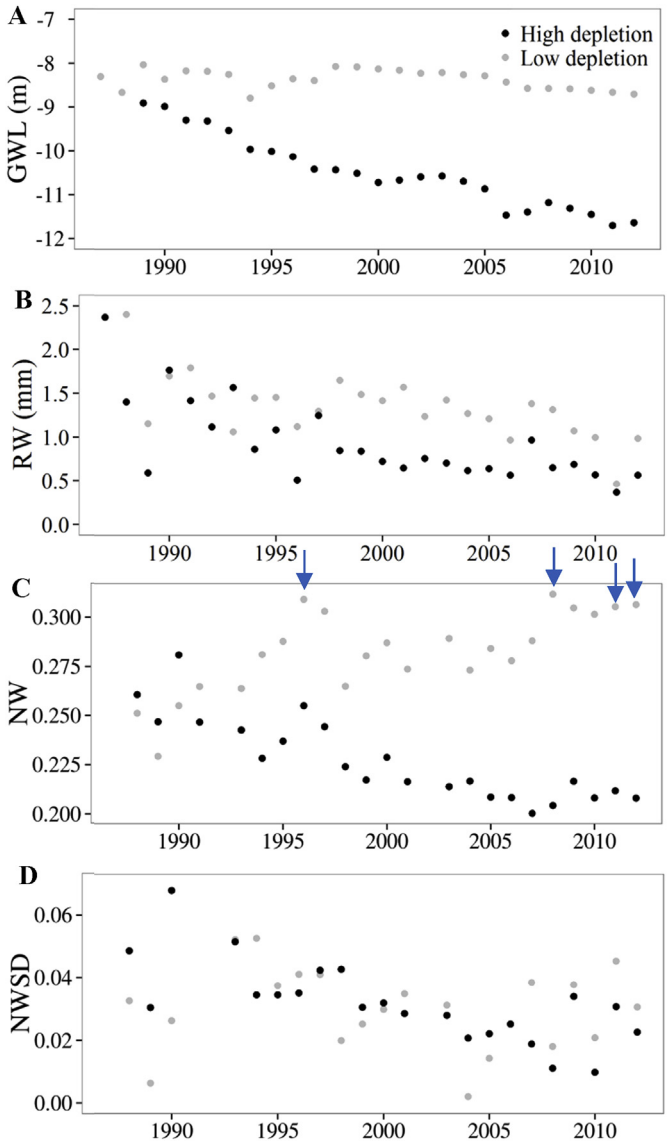

Fig. 3. Time series of stand level variables: (A) Groundwater level (GWL) in metres below ground level.; (B) Average annual ring-width (RW) of viable *P. tamarugo* trees, where mean radial growth was 48% less in the high-depletion site; (C) NDVI in winter (NW); (D) NDVI difference between winter and summer (NWSD). The blue arrows represent the few rainfall events (ranging from 1.6 to 6.9 mm per year) and could explain the small peaks in NW. (For interpretation of the references to colour in this figure legend, the reader is referred to the web version of this article.)

3.2. Annual ring-width and groundwater level (stand level)

Although the *P. tamarugo* tree forms distinct rings with the ring boundaries marked by narrow bands of marginal parenchyma (Fig. 1c), the rings are frequently difficult to discern for various reasons: intra-annual density variations, discontinuous parenchyma bands, or extremely narrow rings, as seen in other tree species (Decuyper et al., 2014). The number of rings detected in the 12 trees investigated ranged from 34 to 39, which is consistent with the estimated age of ca. 41 years (the trees were planted around 1971). As a consequence of the planting method (seedlings of 3–5 months old were planted in 60 cm deep holes below the current soil surface level) (Lanino, 1972), some of the rings from the time series are not visible in our disks since they are only apparent at the

base of the tree (i.e. 60 cm below the soil surface level) explaining the lower number of rings found in this study. The number of tree-rings also supports the assumption that the detected rings are annual, as the number of rings did not exceed the estimated age. Ring-width series measured from different radii of the same tree crossdated well. In some cases crossdating, was obscured by reaction wood formation, especially in the outermost part of the stem. For this reason, the outermost stem parts of the disks, where annual ring boundaries could not be discerned with confidence, were left out of the chronology to avoid introducing possible errors (the rest of the chronology was used and crossdated). Tree-ring series of trees from the two sites showed similar annual variation, with slightly better intercorrelation between trees growing in the low-depletion site (EPS = 0.96; Rbar = 0.79) than between trees growing in the high-depletion site (EPS = 0.83; Rbar = 0.57). All *P. tamarugo* trees exhibited a similar growth trend, with fast juvenile radial growth during the first 10–15 years (which was excluded from the statistical analysis), followed by a sharp reduction to a persistently lower and stable average growth rate of approximately 1 mm per year.

From 1987 to 2012, average annual RW had a significant negative trend over time in trees in both sites, with $p < 0.01$; MKT = −0.520 for the low-depletion site and $p < 0.01$; MKT = −0.586 for the high-depletion site. This is partly attributable to the remaining small ontogenetic trend in all ring-width series. Nevertheless, a comparison between the ring-width chronologies of both sites (Fig. 3b) showed that the ring-width (i.e. the whole time series minus the juvenile phase) was significantly lower by 48% in the high-depletion site compared to the low-depletion site ($U = 135$; $Z = -3.715$; $p < 0.001$).

3.3. NDVI metrics (NW and NWSD) and groundwater level (stand level)

The time-series analysis for the NW showed significant trends for both sites (Table 1) as indicated by the Mann–Kendall trend (MKT) test. In the low-depletion site, NW increased over time ($p < 0.01$; MKT = 0.557), while, in the high-depletion site, NW declined over time ($p < 0.01$; MKT = −0.747; Fig. 3c). The NW was significantly lower when comparing the high-depletion site with the low-depletion site ($U = 20.5$; $Z = -5.361$; $p < 0.001$). NWSD showed no significant positive or negative trend over time in the low-depletion site but a negative trend in the high-depletion site ($p < 0.01$; MKT = −0.573) (Fig 3d). However, when comparing NWSD there were no differences between the two sites ($U = 230.5$; $Z = -0.012$; $p = 0.990$).

In the low-depletion site, the Kendall rank correlation (KRC) indicated that the correlation with the GWL was significantly negative for the NW ($p < 0.05$; KRC = −0.352) and poor for the NWSD ($p < 0.1$; KRC = −0.305). In the high-depletion site, a more significant and positive correlation was found between NW and GWL ($p < 0.01$; KRC = 0.688), and NWSD and GWL ($p < 0.01$; KRC = 0.482), (Table 1).

3.4. Annual ring-width and NDVI metrics (NW and NWSD) (stand level)

The significant negative correlation between RW and NW ($p < 0.01$; KRC = −0.399) in the low-depletion site might be somewhat explained by the slight ontogenetic effect in the RW (see Fig. B in the Supplementary materials), yet there was no correlation between RW and NWSD. Although this ontogenetic effect in the RW is similar in the high-depletion site, there is a significant positive correlation between RW and both NDVI-derived parameters (NW: $p < 0.01$; KRC = 0.420 and NWSD: $p < 0.01$; KRC = 0.457).

3.5. Green Canopy Fraction and groundwater level (tree level)

Although all GCF classes appear in both sites in 2011 (Fig. 4), more trees in the high-depletion site fall within lower GCF classes. There is little difference between sites in the fraction of trees in the lowest GCF class (GCF = 0–25) but in the high-depletion site there are 11% more trees in GCF class 25–50 than in the low-depletion site (Table 2). Only 8% of the trees in the high-depletion site were in GCF class 75–100, compared with 15% in the low-depletion site. The average GCF of all individual trees summarizes the overall difference in GCF between the two sites, which was 0.470 for the high-depletion site and 0.549 for the low-depletion site, and there was a significant difference in GCF values between sites ($U = 1522603.5$; $Z = -8.404$; $p < 0.001$). The standard deviation of GCF was higher in the low-depletion site (i.e. 0.519) than in the high-depletion site (Table 2). In addition to the numerical differences, there are different spatial patterns in the low-depletion site (i.e. the band of trees with a GCF <0.25 and 0.25 to 0.50); in the high-depletion site the GCFs are more homogenous (Fig. 4).

4. Discussion

4.1. Radial stem growth of viable trees is affected by groundwater depletion

Radial growth in the high-depletion site was significantly lower

Table 1
Trends and correlation between stand level variables: groundwater level (GWL, expressed in negative values), ring-width (RW), NDVI measured in winter (NW), and NDVI difference between winter and summer (NWSD) of *P. tamarugo* sites subject to low and high groundwater depletion.

Scenario/parameter	Mann–Kendall trend test	Kendall rank correlation			
		GWL (m)	NW	NWSD	RW (mm)
Low-depletion site					
GWL (m)	−0.348**	–	−0.352**	−0.305*	0.249*
NW	0.557***		–	–	−0.399***
NWSD	NS			–	NS
RW (mm)	−0.520***				–
High-depletion site					
GWL (m)	−0.899***	–	0.688***	0.482***	0.548***
NW	−0.747***		–	–	0.420***
NWSD	−0.573***			–	0.457***
RW (mm)	−0.586***				–

2-sided p value with ***$p < 0.01$, **$p < 0.05$, *$p < 0.1$, NS $p > 0.1$.

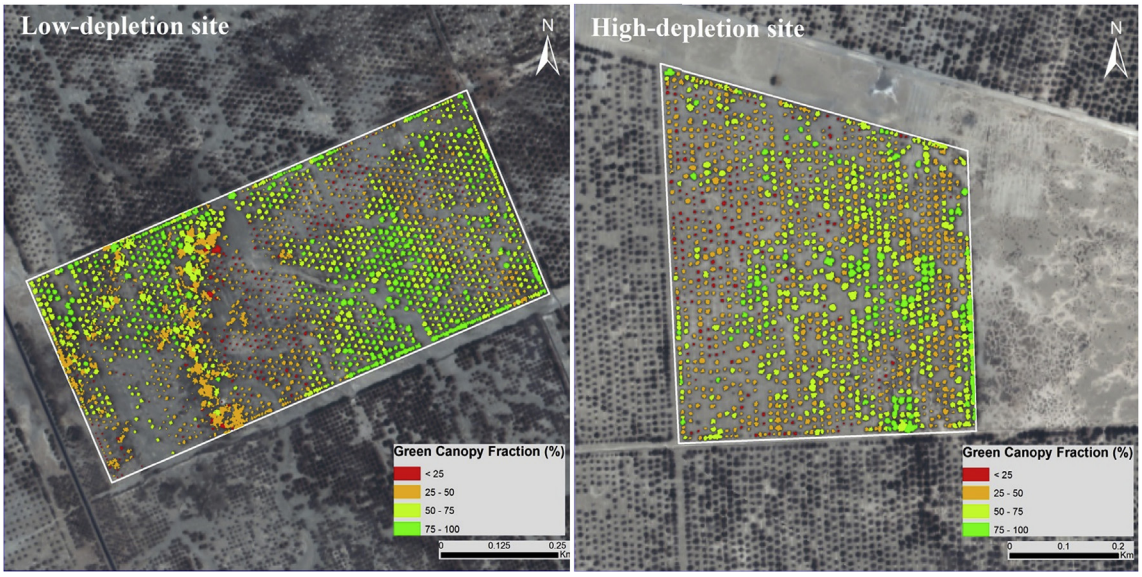

Fig. 4. Green Canopy Fraction (GCF) derived from high-resolution (2.4 m pixel resolution) Worldview2 satellite data (acquired in July 2011).

Table 2
Forest site characteristics of the two study sites. The Green Canopy Fraction (GCF) classes show the percentage of trees organized in four GCF classes. GCF per tree was calculated using the Worldview2 image of July 2011.

Site	Low-depletion site	High-depletion site
CONAF site	Recreo	España
Year planted	1971	1971
Number of trees	2364	1532
Tree density (per ha)	50.3	46.4
Average GCF (SD)	0.549 (0.519)	0.470 (0.185)
GCF class < 25 (%)	9	11
GCF class 25–50 (%)	38	49
GCF class 50–75 (%)	37	32
GCF class 75–100 (%)	15	8

than in the low-depletion site by 48%. The generally slow growth may conceal even greater differences in resource availability between the two sites, In addition, since only viable trees with a GCF class of 75–100 could be sampled for ring-width analyses, it is most likely that overall growth is even lower, as less viable trees have even less growth. A reduction in ring-width was also found in other arid ecosystems where water was limiting growth: for example for *Populus trichocarpa* and *Pinus jeffrey* (Stromberg and Patten, 1990) and for *P. flexuosa* DC. (Giordano et al., 2011). The reduction in ring-width in the high-depletion site may be related to a shift in allocation patterns towards investment of resources into root elongation (Micco and Aronne, 2012; Markesteijn and Poorter, 2009; Chaves et al., 2003). Another possible cause of reduced growth might be reduced carbon fixation due to longer periods of stomatal closure (McDowell et al., 2008). Groundwater depletion may lead to amplification of this potential allocation effect, as seen from the reduced ring-width of the viable trees in the high-depletion site (Fig. 3b). All trees showed high radial growth during the first 10–15 years after establishment. Such a juvenile phase with high height and radial growth is in line with results reported by Rivera et al. (2010), who studied *P. tamarugo* trees in the same region, and by Alvarez et al. (2011) and Villagra et al. (2005) in *P. flexuosa* growing under similarly hyper-arid conditions.

In its natural habitat, *P. tamarugo* trees germinate after major floods which occasionally occur as a result of runoff from the Andes (Mooney et al., 1980). The fast juvenile growth can be an adaptation of these trees to quickly establish and reach the groundwater and in this way avoid premature desiccation when the flood event is over and the high solar radiation prevails (Salih, 1998; Sudzuki, 1985b). Once the tree roots reach the groundwater, allocation strategies may change, with more biomass being invested in maintaining foliage and with root increment being stimulated by drought stress (Markesteijn and Poorter, 2009). Carbon allocation or limited carbon fixation may be the explanation of the relatively low radial increments in the last 20 years in both sites (Fig. 3b). However, further research is needed to understand carbon allocation strategies or limitations in carbon fixation of *P. tamarugo* trees under drought stress.

4.2. Increased drought stress due to groundwater depletion – the remote sensing (crown) perspective

The significant reduction in NW and NWSD of groundwater-dependent *P. tamarugo* trees in the high-depletion site indicates that the trees are experiencing increasing drought stress as a consequence of groundwater depletion. The high evaporative demand in desert areas induces drought stress once the water supply drops below a certain threshold (Houston, 2006). The lower NW and NWSD in the high-depletion site indicate that a drop in groundwater level of about 3 m over the last two decades induced increased drought stress in tree crowns throughout the forest site. The positive correlation between NW, NWSD and GWL could be another indicator showing the detrimental effects of this depletion intensity. Furthermore, the groundwater level in the high-depletion site dropped to 12 m, which according to Chávez et al. (2016) is within the zone (12–20 m) in which a disruption of the water status of the tree occurs. This indicates that most *P. tamarugo* trees in the high-depletion site have had limited access to water (Chávez et al., 2016).

In the low-depletion site, the positive trend in NW suggests that most trees continued to increase their green biomass over time, which is also supported by the negative correlation between NW and GWL (i.e. NW increases due to crown growth, while almost no change is seen in the GWL). The absence of a significant trend in NWSD points to the absence of excessive drought stress, which implies well-functioning pulvinar movement of the leaves during

summer (Chávez et al., 2014). In line with this, GCF was lower in the high-depletion site. A GCF class below 50 indicates trees are unhealthy (Chávez et al., 2016) and 49% of the trees in the high-depletion site belonged to this category (Table 2). Although the GCF is considerably higher in the low-depletion site, the large standard deviation indicates that in addition to healthy trees (high GCF), stressed trees (low GCF) are also present in the tree community here. This, together with the observation of clear spatial patterns in the low-depletion site (Fig. 4), could point to the presence of below-ground features (e.g. bedrock) which define local water availability, e.g. the presence of impenetrable layers or layers hampering root expansion to greater depths to follow the falling groundwater level. Reduced crown vitality (GCF) also means reduced carbon assimilation for root growth and in turn reduces the tree's ability to access declining water reserves. This could also imply that under prevailing drought stress, radial growth is restricted.

4.3. Impact of groundwater depletion on P. tamarugo

All the indicators investigated – GCF, NW, NWSD, and RW – point to a strong effect of groundwater extraction on the viability of the groundwater-dependent *P. tamarugo* tree. Viable trees seem to cope relatively well with falling GWL, but the GCF values show that most of the *P. tamarugo* trees in the high-depletion site were affected by the drop of about 3 m in GWL in the last two decades. This indicates that there is a certain critical threshold of GWL, below which photosynthesis, maintenance of growth and adaptation of root length are constrained. A recent study by Chávez et al. (2016), assessed the GWL of the entire Pampa del Tamarugal and suggested the critical threshold for *P. tamarugo* survival was a depth of 20 m. It is known that other *Prosopis* species can reach groundwater as deep as 50 m (Phillips, 1963). However, when evaluating the adaptive capacity of a species, different factors play an important role, such as initial GWL, extent and speed of GWL depletion, site fertility and impenetrable layers. Our findings suggest that most trees in the high-depletion site are beyond their adaptive capacity and showed signs of stress at a GWL of ~12 m, which is in line with conclusions of Chávez et al. (2016), who showed signs of disruption of the water status in the *P. tamarugo* at this depth. If the current situation remains stable, or GWL continues to fall in response to anthropogenic (pumping) or natural causes, the population will decline. It is clear that the current extraction limitation of 4000 l/s in the Pampa del Tamarugal aquifer is too high for the natural recharge rate of 976 l/s (JICA-DGA-PCI, 1995; Rojas and Dassargues, 2007). Other factors in addition to the anthropogenic pressure that could cause serious and immediate impacts on the *P. tamarugo* population are severe drought and earlier snowmelt or rainfall instead of snow (thus releasing water faster and causing shortages in groundwater supply later in the summer season) in the Andes mountains, due to higher temperatures as described in Coudrain et al. (2005).

4.4. Applicability of a multi-scale approach in arid environments

With this multi-scale approach, the impact of groundwater extraction on groundwater dependent forests was assessed and a methodology for studying the effects on resource acquisition (canopy) and radial growth was demonstrated. Although only one very high-resolution satellite image for deriving data at tree level (GCF) was used, the results show the potential of this approach for future studies. For example, the increasing use of drones and the upcoming high spatial and/or temporal resolution satellites with higher spectral resolution, such as Worldview3 (spatial resolution of 2 m and eight spectral bands) and Sentinel 2 (free access, spatial resolution: 10 m and five days' revisit time) will increase possibilities to study ecosystems throughout the year and to combine this data with ground-based measurements at tree level. Arid ecosystems have the advantage of being infrequently covered by clouds, which leads to more cloud free and higher quality (e.g. less aerosols) satellite data, as was the case in the Atacama Desert.

To date, the combination of remotely-sensed indices with dendrochronology of tropical trees has not been sufficiently explored. One of the few studies showed that shifts in regional precipitation patterns could be explained by combining tree-ring chronologies and remotely-sensed data (Southworth et al., 2013). In the present paper, the results provided insight into what can be seen from the canopy and within the tree (i.e. radial growth) in trees undergoing drought stress (see Table 1, NW, NWSD and RW).

5. Conclusions

We conclude that *P. tamarugo* trees were affected by the drop in groundwater of about 3 m (from ~8 to 12 m) in recent decades. Groundwater depletion increases drought stress in the tree canopy and reduces radial growth, even in viable trees. Although viable trees can currently cope with this level of groundwater depletion, they could experience a reduction carbon fixation or may allocate more resources towards root elongation in order to remain in contact with the groundwater (this could be a possible explanation of the higher reduction in radial growth in the high depletion site). Furthermore, the drought-stress symptoms, detected by GCF on tree level, and NW and NWSD on stand level in the high-depletion site suggest that the viability of this whole stand is declining. If groundwater extraction continues in the Atacama Desert at the same rate, this unique tree species may not persist. In order to curb this trend, groundwater extraction rates should decrease drastically or should be spread both spatially and temporally so that the *P. tamarugo* stands have more time to adjust to lower soil water levels. The combination of remote sensing and tree-ring analysis provides a relevant insight into the ecophysiology of this desert tree, by assessing crown and stem status, and shows potential for upscaling drought effects from trees to stands and perhaps basins.

Acknowledgements

We thank the Alberta Mennega foundation, Beca CONICYT-Wageningen, and Fondo Basal FONDECYT FB-002 (linea 4) for providing financial support. We are grateful to the Ministry of Agriculture - CONAF (Government of Chile) for granting access to the sites, Mauricio Ortiz for his valuable knowledge on leaf phenology, Cristian Riquelme for logistic support, and the Universidad Arturo Prat for providing climatic data from the Canchones experimental station. The discussion improved from exchange of ideas with colleagues from the COST FP1106 network. We are indebted to Digital Globe for the Quickbird2 and Worldview2 imagery and to NASA for the Landsat images. We are also grateful to the editor Cristina Armas, the anonymous reviewers and Sarah Carter for their useful remarks improving the paper. Professional language editing was provided by Joy Burrough.

Appendix A. Supplementary data

Supplementary data related to this article can be found at http://dx.doi.org/10.1016/j.jaridenv.2016.03.014.

References

Acevedo, E., Pastenes, J., 1983. Distribución de *Prosopis tamarugo* Phil. en la Pampa del Tamarugal (Desierto de Atacama). Terra Arid. 2, 317–333.

Altamirano, H., 2006. *Prosopis tamarugo* Phil. Tamarugo. In: Donoso, C. (Ed.), Las Especies Arbóreas de Los Bosques Templados de Chile Y Argentina, Autoecología. Marisa Cuneo Ediciones, Valdivia, Chile, pp. 534–540.

Alvarez, J. a., Villagra, P.E., Villalba, R., Cony, M. a., Alberto, M., 2011. Wood productivity of *Prosopis flexuosa* D.C. woodlands in the central Monte: influence of population structure and tree-growth habit. J. Arid. Environ. 75, 7–13. http://dx.doi.org/10.1016/j.jaridenv.2010.09.003.

Aravena, 1996. Isotope hydrology and geochemistry of northern Chile groundwaters. Bull. – Inst. Fr. d'Etudes Andin. 24, 495–503.

Bogino, S.M., Jobbágy, E.G., 2011. Climate and groundwater effects on the establishment, growth and death of *Prosopis caldenia* trees in the Pampas (Argentina). For. Ecol. Manag. 262, 1766–1774. http://dx.doi.org/10.1016/j.foreco.2011.07.032.

Botti, C., Sudzuki, F., 1970. Relaciones hídricas del tamarugo (*Prosopis tamarugo* Phil) en la localidad de Canchones. Santiago, Chile.

Briner, C., 1985. Phenotypic characterization of the tamarugo biotypes at the Tamarugal Pampa. In: Habit, M. (Ed.), The Current State of Knowledge on Prosopis Tamarugo. FAO, Rome, Italy.

Bunn, A.G., 2008. A dendrochronology program library in R (dplR). Dendrochronologia 26, 115–124. http://dx.doi.org/10.1016/j.dendro.2008.01.002.

Burkart, A., 1976. A monograph of the genus *Prosopis* (Leguminosae subfam Mimosoideae), catalogue of the recognized species of Prosopis. J. Arnold Arbor. 57, 219–249, 450–525.

Chaves, M.M., Maroco, J.P., Pereira, J.S., 2003. Understanding plant responses to drought—from genes to the whole plant. Funct. Plant Biol. 30, 239–264.

Chávez, R.O., Clevers, J.G.P.W., 2012. Worldview2 Imagery for Assessing Health Condition of Desert Trees. Wageningen.

Chávez, R.O., Clevers, J.G.P.W., Decuyper, M., De Bruin, S., Herold, M., 2016. 50 years of groundwater extraction in the Pampa del Tamarugal basin: can Tamarugo trees survive in the hyper-arid Atacama Desert? J. Arid. Environ. 124, 292–303. http://dx.doi.org/10.1016/j.jaridenv.2015.09.007.

Chávez, R.O., Clevers, J.G.P.W., Herold, M., Acevedo, E., Ortiz, M., 2013a. Assessing water stress of desert Tamarugo trees using in situ data and very high spatial resolution remote sensing. Remote Sens. 5, 5064–5088. http://dx.doi.org/10.3390/rs5105064.

Chávez, R.O., Clevers, J.G.P.W., Herold, M., Ortiz, M., Acevedo, E., 2013b. Modelling the spectral response of the desert tree prosopis tamarugo to water stress. Int. J. Appl. Earth Obs. Geoinf. 21, 53–65. http://dx.doi.org/10.1016/j.jag.2012.08.013.

Chávez, R.O., Clevers, J.G.P.W., Verbesselt, J., Naulin, P.I., Herold, M., 2014. Detecting leaf pulvinar movements on NDVI time series of desert trees: a new approach for water stress detection. PLoS One 9, e106613. http://dx.doi.org/10.1371/journal.pone.0106613.

CIDERH, 2013. Recursos hídricos de la región de Tarapacá. Diagnóstico y sistematización de la información. Universidad Arturo Prat, Iquique, Chile.

CONAF, 1997. Plan de manejo reserva nacional Pampa del Tamarugal. Corporación Nacional Forestal (CONAF), Santiago, Chile.

Cooper, D.J., D'Amico, D.R., Scott, M.L., 2003. Physiological and morphological response patterns of *Populus deltoides* to alluvial groundwater pumping. Environ. Manag. 31, 215–226. http://dx.doi.org/10.1007/s00267-002-2808-2.

Coudrain, A., Francou, B., Kundzewicz, Z.W., 2005. Glacier shrinkage and water resources in the Andes. Eos Trans. Am. Geophys. Union. http://dx.doi.org/10.1029/2005EO430005.

De Beurs, K.M., Henebry, G.M., 2005. A statistical framework for the analysis of long image time series. Int. J. Remote Sens. 26, 1551–1573. http://dx.doi.org/10.1080/01431160512331326657.

Decuyper, M., Cornelissen, P., Sass-Klaassen, U., 2014. Establishment and growth of hawthorn in floodplains in the Netherlands. Dendrochronologia 32, 173–180. http://dx.doi.org/10.1016/j.dendro.2014.04.002.

DICTUC, 2008. Anexo VIII.2 Modelación de la Evolución del Nivel de la Napa en la Pampa del Tamarugal. In: EIA Proyecto Pampa Hermosa. Dirección de Investigaciones Científicas y Tecnológicas Universidad Católica de Chile, Santiago, Chile, p. 169.

DICTUC, 1988. Modelo de simulación hidrogeológico de la Pampa del Tamarugal (Hydrogeological simulation model of the Pampa del Tamaruga). Santiago, Chile.

Eamus, D., Zolfaghar, S., Villalobos-Vega, R., Cleverly, J., Huete, a., 2015. Groundwater-dependent ecosystems: recent insights, new techniques and an ecosystem-scale threshold response. Hydrol. Earth Syst. Sci. Discuss. 12, 4677–4754. http://dx.doi.org/10.5194/hessd-12-4677-2015.

Ehleringer, J., Forseth, I., 1980. Solar tracking by plants. Science 210, 1094–1098. http://dx.doi.org/10.1126/science.210.4474.1094.

Favier, V., Falvey, M., Rabatel, A., Praderio, E., López, D., 2009. Interpreting discrepancies between discharge and precipitation in high-altitude area of Chile's Norte Chico region (26-32°S). Water Resour. Res. 45 http://dx.doi.org/10.1029/2008WR006802 n/a–n/a.

February, E.C., Higgins, S.I., Newton, R., West, A.G., 2007. Tree distribution on a steep environmental gradient in an arid savanna. J. Biogeogr. 34, 270–278. http://dx.doi.org/10.1111/j.1365-2699.2006.01583.x.

Gascoin, S., Kinnard, C., Ponce, R., Lhermitte, S., MacDonell, S., Rabatel, A., 2011. Glacier contribution to streamflow in two headwaters of the Huasco River, dry Andes of Chile. Cryosph 5, 1099–1113. http://dx.doi.org/10.5194/tc-5-1099-2011.

Giantomasi, M.A., Roig-Juñent, F.A., Villagra, P.E., 2013. Use of differential water sources by *Prosopis flexuosa* DC: a dendroecological study. Plant Ecol. 214, 11–27. http://dx.doi.org/10.1007/s11258-012-0141-2.

Giordano, C.V., Guevara, A., Boccalandro, H.E., Sartor, C., Villagra, P.E., 2011. Water status, drought responses, and growth of *Prosopis flexuosa* trees with different access to the water table in a warm South American desert. Plant Ecol. 212, 1123–1134. http://dx.doi.org/10.1007/s11258-010-9892-9.

Grissino-Mayer, H.D., 2001. Evaluating crossdating accuracy: a manual and tutorial for the computer program COFECHA. Tree-Ring Res. 57.

Groom, B.P.K., Froend, R.H., Mattiske, E.M., 2000. Impact of groundwater abstraction on a Banksia woodland, Swan Coastal Plain, Western Australia. Ecol. Manag. Restor. 1, 117–124. http://dx.doi.org/10.1046/j.1442-8903.2000.00033.x.

Habit, M.A., Contreras, T.D., Gonzalez, R.H., 1981. Prosopis Tamarugo: Fodder Tree for Arid Zones. FAO Plant Protection Paper 25, Rome, Italy.

Hipel, K.W., McLeod, A.I., 1994. Time Series Modelling of Water Resources and Environmental Systems. Elsevier, Amsterdam, The Netherlands.

Holmes, R.L., 1983. Computer assisted quality control in tree ring dating and measurement. Tree-Ring Bull. 43, 69–78.

Houston, J., 2006. Evaporation in the Atacama Desert: an empirical study of spatio-temporal variations and their causes. J. Hydrol. 330, 402–412. http://dx.doi.org/10.1016/j.jhydrol.2006.03.036.

Houston, J., Hartley, A.J., 2003. The central andean west-slope rainshadow and its potential contribution to the origin of hyper-aridity in the Atacama Desert. Int. J. Climatol. 23, 1453–1464. http://dx.doi.org/10.1002/joc.938.

JICA-DGA-PCI, 1995. The Study on the Development of Water Resources in Northern Chile (Technical reports, Supporting reports B and C. Santiago, Chile).

Jobbágy, E.G., Nosetto, M.D., Villagra, P.E., Jackson, R.B., 2011. Water subsidies from mountains to deserts: their role in sustaining groundwater-fed oases in a sandy landscape. Ecol. Appl. 21, 678–694. http://dx.doi.org/10.1890/09-1427.1.

Lanino, I., 1972. General Instructions for Sowing and Planting Tamarugo. Rome, Italy.

López, B.C., Holmgren, M., Sabaté, S., Gracia, C. a., 2008. Estimating annual rainfall threshold for establishment of tree species in water-limited ecosystems using tree-ring data. J. Arid. Environ. 72, 602–611. http://dx.doi.org/10.1016/j.jaridenv.2007.10.012.

López, B.C., Sabaté, S., Gracia, C. a., Rodríguez, R., 2005. Wood anatomy, description of annual rings, and responses to ENSO events of *Prosopis pallida* H.B.K., a widespread woody plant of arid and semi-arid lands of Latin America. J. Arid. Environ. 61, 541–554. http://dx.doi.org/10.1016/j.jaridenv.2004.10.008.

Markesteijn, L., Poorter, L., 2009. Seedling root morphology and biomass allocation of 62 tropical tree species in relation to drought- and shade-tolerance. J. Ecol. 97, 311–325. http://dx.doi.org/10.1111/j.1365-2745.2008.01466.x.

Masek, J.G., Vermote, E.F., Saleous, N.E., Wolfe, R., Hall, F.G., Huemmrich, K.F., Gao, F., Kutler, J., Lim, T.K., 2006. A landsat surface reflectance dataset for North America, 1990-2000. IEEE Geosci. Remote Sens. Lett. 3, 68–72. http://dx.doi.org/10.1109/LGRS.2005.857030.

McDowell, N., Pockman, W.T., Allen, C.D., Breshears, D.D., Cobb, N., Kolb, T., Plaut, J., Sperry, J., West, A., Williams, D.G., Yepez, E.A., 2008. Mechanisms of plant survival and mortality during drought: why do some plants survive while others succumb to drought? New Phytol. 178, 719–739. http://dx.doi.org/10.1111/j.1469-8137.2008.02436.x.

McKay, C.P., Friedmann, E.I., Gómez-Silva, B., Cáceres-Villanueva, L., Andersen, D.T., Landheim, R., 2003. Temperature and moisture conditions for life in the extreme arid region of the Atacama Desert: four years of observations including the El Niño of 1997-1998. Astrobiology 3, 393–406. http://dx.doi.org/10.1089/153110703769016460.

Micco, V. De, Aronne, G., 2012. Morpho-anatomical traits for plant adaptation to drought. In: Aroca, R. (Ed.), Plant Responses to Drought Stress. Springer-Verlag, Berlin Heidelberg, pp. 37–61. http://dx.doi.org/10.1007/978-3-642-32653-0.

Mooney, H.A., Gulmon, S.L., Rundel, P.W., Ehleringer, J., 1980. Further observations on the water relations of *Prosopis tamarugo* of the northern Atacama desert. Oecologia 44, 177–180. http://dx.doi.org/10.1007/BF00572676.

Naumburg, E., Mata-Gonzalez, R., Hunter, R.G., McLendon, T., Martin, D.W., 2005. Phreatophytic vegetation and groundwater fluctuations: a review of current research and application of ecosystem response modeling with an emphasis on great basin vegetation. Environ. Manag. 35, 726–740. http://dx.doi.org/10.1007/s00267-004-0194-7.

Navarro-González, R., Rainey, F. a, Molina, P., Bagaley, D.R., Hollen, B.J., de la Rosa, J., Small, A.M., Quinn, R.C., Grunthaner, F.J., Cáceres, L., Gomez-Silva, B., McKay, C.P., 2003. Mars-like soils in the Atacama Desert, Chile, and the dry limit of microbial life. Science 302, 1018–1021. http://dx.doi.org/10.1126/science.1089143.

Ortiz, M., Silva, P., Acevedo, E., 2010. Leaf Water Parameters in *Prosopis tamarugo* Phil. Subject to a Lowering of the Water Table (Nivel freático en la Pampa del Tamarugal y crecimiento de *Prosopis tamarugo* Phil). Universidad de Chile.

Pastenes, C., 2004. Leaf movements and photoinhibition in relation to water stress in field-grown beans. J. Exp. Bot. 56, 425–433. http://dx.doi.org/10.1093/jxb/eri061.

Phillips, W., 1963. Depth of roots in soil. Ecology 44, 424. http://dx.doi.org/10.2307/1932198.

Rivera, M. a, R., J.M., Shea, D.E., 2010. Dendrocronología en la Pampa del Tamarugal, Desierto de Atacama, Norte de Chile. Diálogo Andin. 36, 33–50.

Rojas, R., Batelaan, O., Feyen, L., Dassargues, A., 2010. Assessment of conceptual model uncertainty for the regional aquifer Pampa del Tamarugal – North Chile. Hydrol. Earth Syst. Sci. Discuss. http://dx.doi.org/10.5194/hessd-6-5881-2009.

Rojas, R., Dassargues, A., 2007. Groundwater flow modelling of the regional aquifer of the Pampa del Tamarugal, northern Chile. Hydrogeol. J. 15, 537–551. http://dx.doi.org/10.1007/s10040-006-0084-6.

Salih, a a, 1998. Root and shoot growth of *Prosopis chilensis* in response to soil

impedance and soil matric potential. J. Arid. Env. 40, 43–52. http://dx.doi.org/10.1006/jare.1998.0426.
Southworth, J., Rigg, L., Gibbes, C., Waylen, P., Zhu, L., Mccarragher, S., Cassidy, L., 2013. Integrating dendrochronology, climate and satellite remote sensing to better understand savanna landscape dynamics in the Okavango Delta, Botswana. Land 2, 637–655. http://dx.doi.org/10.3390/land2040637.
Stock, W.D., Bourke, L., Froend, R.H., 2012. Dendroecological indicators of historical responses of pines to water and nutrient availability on a superficial aquifer in south-western Australia. For. Ecol. Manag. 264, 108–114. http://dx.doi.org/10.1016/j.foreco.2011.09.033.
Stromberg, J.C., Patten, D.T., 1990. Riparian vegetation instream flow requirements: a case study from a diverted stream in the Eastern Sierra Nevada, California, USA. Environ. Manag. 14, 185–194. http://dx.doi.org/10.1007/BF02394035.
Stromberg, J.C., Tiller, R., Richter, B., 1996. Effects of groundwater decline on riparian vegetation of semiarid regions: the San Pedro, Arizona. Ecol. Appl. 6, 113–131. http://dx.doi.org/10.2307/2269558.
Sudzuki, F., 1985a. Environmental moisture utilization by *Prosopis tamarugo* (Phil.). In: Habit, M.A. (Ed.), The Current State of Knowledge on *Prosopis tamarugo*. FAO, Rome, Italy.
Sudzuki, F., 1985b. Environmental influence on foliar anatomy of *Prosopis tamarugo* Phil. In: Habit, M.A. (Ed.), The Current State of Knowledge on *Prosopis tamarugo*. FAO, Rome, Italy.
Villagra, P.E., Roig, J.F.A., 1997. Wood structure of *Prosopis alpataco* and *P. Argentina* growing under different edaphic conditions. IAWA J. 18, 37–51. http://dx.doi.org/10.1163/22941932-90001458.
Villagra, P.E., Villalba, R., Boninsegna, J. a, 2005. Structure and growth rate of *Prosopis flexuosa* woodlands in two contrasting environments of the central Monte desert. J. Arid. Environ. 60, 187–199. http://dx.doi.org/10.1016/j.jaridenv.2004.03.016.
Villalba, R., 1985. Xylem structure and cambial activity in *Prosopis flexuosa* DC. IAWA Bull. 6, 119–130. http://dx.doi.org/10.1163/22941932-90000923.
Villalba, R., Boninsegna, J.A., 1989. Dendrochronological studies on *Prosopis flexuosa* DC. Growth rings Trop. trees 10, 155–160. doi:10.1163/22941932-90000483.
Wigley, T.M.L., Briffa, K.R., Jones, P.D., 1984. On the average value of correlated time series, with applications in dendroclimatology and hydrometeorology. J. Clim. Appl. Meteorol. http://dx.doi.org/10.1175/1520-0450, 023<0201:OTAVOC>2.0.CO;2.
Zencich, S.J., Froend, R.H., Turner, J.V., Gailitis, V., 2002. Influence of groundwater depth on the seasonal sources of water accessed by Banksia tree species on a shallow, sandy coastal aquifer. Oecologia 131, 8–19. http://dx.doi.org/10.1007/s00442-001-0855-7.